



ORIGINAL ARTICLE

Effect of carbon nanotubes on Portland cement matrices

Efeito de nanotubos de carbono em matriz de cimento Portland

Thiago Melanda Mendes^a

Marcelo Henrique Farias de Medeiros^b

^aUniversidade Tecnológica Federal do Paraná – UTFPR, Departamento de Engenharia Ambiental, Londrina, PR, Brasil

^bUniversidade Federal do Paraná – UFPR, Departamento de Engenharia Civil, Programa de Pós-graduação em Engenharia Civil – PPGECC, Curitiba, PR, Brasil

Received 20 September 2022

Accepted 17 December 2022

Abstract: This study evaluates the effects of three carbon nanotubes with different geometric characteristics on the rheological behaviour and mechanical performance, as well as on the microstructure of mortars and cement pastes. For nanotube content ranging from 0.025 to 0.2 wt%, the yield stress and viscosity were determined by rotational rheometry, and mechanical performance was evaluated by flexural strength and dynamic modulus of elasticity. The microstructural analysis was performed by X-ray diffraction, thermo-gravimetric analysis and scanning electron microscopy (SEM). The obtained results showed that the yield stress presents a considerable increase as the carbon nanotube content increases. The viscosity was also influenced by the presence of carbon nanotubes. The flexural strength of mortars increases for different amounts of carbon nanotubes, and depending on the geometric characteristics of the carbon nanotubes, the material behaves like a composite. The microstructural analysis showed the nucleation of hydration products on the surface of the carbon nanotubes, and that the better mechanical performance of matrices containing carbon nanotubes is not related to the increase in hydration products.

Keywords: rheological properties, mechanical properties, x-ray diffraction, thermo-gravimetry, scanning electron microscopy.

Resumo: este estudo avaliou os efeitos de três nanotubos de carbono com diferentes características geométricas no comportamento reológico e desempenho mecânico, assim como na microestrutura de argamassas e pastas de cimento. Para teores de nanotubos de carbono variando de 0,025 a 0,2%, a tensão de escoamento e a viscosidade foram determinadas por meio de reometria rotacional, e o desempenho mecânico foi avaliado através da resistência à flexão e módulo de elasticidade dinâmico. A análise microestrutural foi conduzida através da difração de raios-X, análise termogravimétrica, e microscopia eletrônica de varredura. Os resultados obtidos mostram que a tensão de escoamento apresenta um aumento considerável com o aumento no teor de nanotubos. E a viscosidade também é influenciada pela presença dos nanotubos de carbono. A resistência à flexão das argamassas aumenta para os diferentes teores de nanotubos de carbono. E dependendo das características geométricas dos nanotubos, o material se comporta como um compósito. A análise microestrutural mostrou a nucleação de produtos de hidratação sobre a superfície dos nanotubos de carbono, e que o melhor desempenho mecânico das matrizes contendo nanotubos de carbono não está relacionada com o aumento dos produtos de hidratação.

Palavras-chave: comportamento reológico, desempenho mecânico, difração de raios-X, análise termogravimétrica, microscopia eletrônica de varredura.

How to cite: T. M. Mendes and M. H. F. Medeiros, “Effect of carbon nanotubes on Portland cement matrices,” *Rev. IBRACON Estrut. Mater.*, vol. 16, no. 5, e16508, 2023, <https://doi.org/10.1590/S1983-41952023000500008>

1 INTRODUCTION

The use of carbon nanotubes is a recent practice. The first studies were developed in the 20th century and published by Li et al. [1] and Yakovlev et al. [2]. Since this research, interest in this topic has increased considerably. The

Corresponding author: Thiago Melanda Mendes. E-mail: thiagomendes@utfpr.edu.br

Financial support: Araucaria Foundation 668/2014, CNPq – 152200/2019-3.

Conflict of interest: Nothing to declare.

Data Availability: The data that support the findings of this study are available from the corresponding author, T. M. Mendes, upon reasonable request.

This is an Open Access article distributed under the terms of the Creative Commons Attribution License, which permits unrestricted use, distribution, and reproduction in any medium, provided the original work is properly cited.

rheological behaviour of cement-based materials is directly affected by the incorporation of carbon nanotubes. An increase in viscosity of cement pastes due to the incorporation of the same type of carbon nanotubes was demonstrated by Konsta-Gdoutos et al. [3]. A linear increase in yield stress was published by Andrade et al. [4], Reales et al. [5], [6], and Batiston et al. [7] for cement based-material pastes formulated with a carbon nanotube content of less than 0.2 wt%. For larger amounts of carbon nanotubes, Medeiros et al. [8] and Jiang et al. [9] observed an exponential increase in yield stress for mixtures containing up to 0.5 wt% of carbon nanotubes.

Many studies have evaluated the effect of the same type of carbon nanotubes with and without functionalization on mechanical performance of cement-based materials. However, only some of the available references evaluated the geometric characteristics of carbon nanotubes: the diameter was kept constant and the length varied by Konsta-Gdoutos et al. [10], Musso et al. [11], Al-Rub et al. [12] and Chen et al. [13]. While the length was kept constant and the diameter of carbon nanotubes was changed in the studies developed by Collins et al. [14] and Gao et al. [15]. The diameter and length were both varied in studies published by Sobolkina et al. [16], Souza et al. [17], Hawreen [18], [19] and Manzur et al. [20].

Considering that the effect of carbon nanotubes on mechanical performance of cement-based materials is a microstructure response, the mechanisms of these fibers in cementitious matrices were discussed by Fehervari et al. [21], Chen et al. [22] and Ramezani et al. [23]. Chen et al. [22] showed that part the carbon nanotubes can adsorb on the surface of cement particles, and part of them can perform as a reinforcing material. The improvement in the strength of mortars formulated with a low content of carbon nanofibers (< 1 wt%) was not related to the increase in hydration products or the reduction of porosity as published by Fehervari et al. [21]. Thus, this paper aims to study the effect of carbon nanotubes with different geometric characteristics on rheological behaviour, mechanical performance and cementitious matrix microstructure.

2 MATERIALS AND EXPERIMENTAL PROGRAM

Three different aqueous suspensions of multi-walled carbon nanotubes (MWCNT) were obtained from Nano Amorphous Materials. They were called CNT₁, CNT₂ and CNT₃, and their characteristics are listed in Table 1. According to the supplier procedures, the carbon nanotubes were dispersed using a combination of 90 wt% of aromatic modified polyethylene glycol ether (PEG) and 10 wt% of water. The amount of dispersing agent present in each product can be calculated (Nanoamor, 2022). According to information provided by the supplier, the diameter and length of different samples of carbon nanotubes was obtained from High Resolution Transmission Electron Microscopy and Raman spectroscopy.

Table 1 – Physical characteristics of MWCNT suspensions [2]

Description	CNT ₁	CNT ₂	CNT ₃
Diameter (nm)	> 50	20-30	30-50
Length (μm)	10-20	10-30	10-20
Specific surface area (m ² /g)	43.00	39.38	55.94
Density (g/cm ³)	2.10	2.10	2.10
Solids concentration (wt%)	7-8	3	1
*CNT/water dispersant	1.7%	1.3%	1.1%
Water dispersant concentration (mmol/l)	1.78	0.559	0.154

The specific surface area was measured by gas adsorption (B.E.T). Samples were dried in an oven at 105°C and kept under a vacuum of 68.9 pascal at 60°C for 24 hours. The density of carbon nanotubes was obtained from the supplier. Table 2 presents the physical-chemical characteristics of Portland cement type CPV-ARI, equivalent to type III cement [24]. Chemical composition was determined by X-ray fluorescence in an unpressed sample, using the EDX 750 Shimadzu equipment. Lignosulfonate-based superplasticizer was used as a dispersing additive. The particle size distributions of carbon nanotubes and Portland cement CPV-ARI were determined with a Malvern 2200 laser granulometer, which was also used to evaluate the granulometry of carbon nanotubes by Yakovlev et al. [25], and Krause et al. [26] for carbon nanotubes in dry powder condition. Transmission Electron Microscopy (TEM) of carbon nanotube suspensions was carried out with Fei Tecnai G2 equipment, operating at 80 and 120 kV. The samples of nanotube suspensions were diluted to 1 mg/ml. Five milliliters (5μl) of these diluted suspensions were placed on a copper-carbon grid (300 mesh) and covered with Formvar.

Figure 1 shows the Portland cement diffractogram and the main phases were identified: Alite (C₃S) – 3CaO.SiO₂, Belite (C₂S) – 2CaO.SiO₂, Gypsum - Ca.SO₄.1/2H₂O and Calcium hydroxide - Ca(OH)₂ [27], as well as the aluminum oxide (Al₂O₃) peaks at $2\theta = 25.5, 35.15, 43.35^\circ$. The presence of Arkanite – K₂SO₄, and Langbeinite – K₂Mg₂(SO₄)₃ phosphates phases was identified considering their peaks at $2\theta = 30.78^\circ$ and 31.02° , respectively. The chemical analysis

of cement (Table 2) did not reveal the presence of aluminum oxide, which does not allow the formation of Tricalcium aluminate (C_3A) and was not identified in X-ray diffraction considering its main peaks at $2\theta = 20.95^\circ$ and 33.25° .

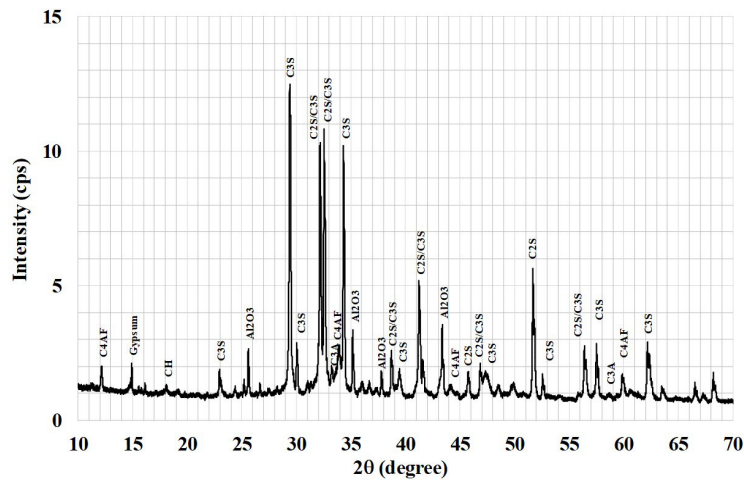


Figure 1. Diffractogram of Portland cement CPV-ARI

The presence of tetra-calcium ferro-aluminate (C_4AF) – $4CaO \cdot Al_2O_3 \cdot Fe_2O_3$ can be replaced by tetra calcium ferrite, $4CaO \cdot Fe_2O_3$, as iron ions can take the place of aluminum ions in a crystalline structure of C_4F [27]. Chemical analysis also revealed a considerable percentage of potassium oxide, 5.87% of K_2O . This is even considering that the amount of this element was combined in sulfate phase, for example, the Arkanite K_2SO_4 . There is only 0.693% of SO_3 according to the chemical analysis, which can represent an amount around 1.5% of K_2SO_4 . Thus, subtracting the percentage of 0.816% of K_2O chemically bounded in the sulfate phase, there is 5.05% of K_2O which must be chemically bounded with the clinker phases. Taylor [27] reported that Woermann et al. found that up to 1.4% of Na_2O or K_2O can be incorporated into C_3S , where the sodium and potassium ions can replace calcium ions. Or even a type of belite phase compound (Glascrite) $KC_{23}S_{12}$ can be used, which contains 3.5% of potassium

Table 2 – Physical-chemical characteristics of Portland cement

Description	CaO	SiO ₂	K ₂ O	Fe ₂ O ₃	SO ₃
Chemical composition (%)	65.01	22.62	5.86	5.05	0.69
Lost in ignition (%)				6.61	
Specific surface Area (m ² /g)				1.419	
Density (g/cm ³)				2.99	

A reference mixture without carbon nanotubes, and mixtures formulated with 0.025, 0.05, 0.1 and 0.2 wt% of CNT_1 , CNT_2 and CNT_3 were evaluated. The lignosulfonate-based dispersant content was fixed at 1 wt.% of solids, and the water/solids ratio of 0.375 was kept constant. For all mixtures, the water content of the dispersant and carbon nanotube suspensions was subtracted from the total amount. For mortars, the cement:sand ratio was fixed at 1:1. In order to consider the possible influence of the amount of polyethylene glycol on the evaluated properties, the concentration of this dispersing agent in each formulation was calculated, whose values are listed in Table 3.

The suspensions of carbon nanotubes and the dispersant were previously diluted in deionized water. The mixing was carried out in a laboratory planetary mixer, applying the following process: (i) the dry powder was mixed at 60 rpm for 60s; (ii) 2/3 of suspension (water + dispersant) was added and mixed at 60 rpm for 120s; (iii) 1/3 of suspension was added (water + carbon nanotubes) and mixed at 60 rpm for 120s. Contents ranging from 600 to 650g were mixed for each batch. A temperature-controlled rheometer with Vane geometry with a diameter of 15 mm and a height of 30 mm was used to measure the rheological properties of pastes. Flow curves were obtained using a shear rate control, ranging from 10 to 100 s⁻¹, in 10 s⁻¹ intervals. The shear rate (γ) was increased from 10 to 100 s⁻¹ (upper curve) and reduced from 100 to 10 s⁻¹ (downs curve). The pastes were held for 30 seconds at each shear rate and the values were recorded

in the last 3 seconds. The yield stress (τ_0) and the plastic viscosity (η) were calculated using the Bingham Equation ($\tau = \tau_0 + \eta * \gamma$), considering the upper-steps curve. All rotational rheometry tests were performed at 23°C after 5 minutes of adding water to the powder.

Table 3 - Mixtures

Properties	Cement (g)	Suspension of CNT (g)	PEG (mmol)	Water (L)	Concentration (mmol/L)
Reference	300	0	0	0.1125	0
0.025% CNT ₁	300	1.07	1.907	0.1125	16.95
0.05% CNT ₁	14.35	2.14	3.814	0.1125	33.90
0.1% CNT ₁	18.02	4.28	7.628	0.1125	67.80
0.2% CNT ₁	22.27	8.57	15.257	0.1125	135.6
0.025% CNT ₂	19.42	2.5	1.398	0.1125	12.42
0.05% CNT ₂	45.46	5	2.796	0.1125	24.85
0.1% CNT ₂	32.44	10	5.593	0.1125	49.71
0.2% CNT ₂	32.52	20	11.186	0.1125	99.42
0.025% CNT ₃	21.71	7.5	1.159	0.1125	10.30
0.05% CNT ₃	18.76	15	2.318	0.1125	20.60
0.1% CNT ₃	19.16	30	4.637	0.1125	41.21
0.2% CNT ₃	47.96	60	9.274	0.1125	82.43

Six prismatic samples (1.6x4x16cm) of mortars were molded; compaction was applied to avoid molding defects. The samples were kept at 23°C for 24 hours and immersed in a saturated calcium hydroxide solution at 23°C for 7 days. The flexural strength of mixtures was measured on six prismatic samples, which had the upper face milled to remove surface irregularities. The flexural strength was measured using a universal testing machine applying a strain rate of 0.1 mm/s. The dynamic modulus of elasticity was measured according to standard procedure [28].

For the microstructural analysis, the inner part of the paste sample was extracted, which was maintained under the same curing conditions described above. For X-ray diffraction and thermogravimetric analysis, the samples were ground and sieved through 200 mesh (0.075 mm). The diffractogram of samples was obtained in a Buckler X-ray diffractometer operating at 30 kV and 10 mA, with a copper tube, from 10 to 70° at 0.01°/s. Thermogravimetric analysis was performed from 100 to 950°C with a heating rate of 10°C/min in an alumina crucible, with a nitrogen flow of 20 ml/min. The microstructure of the samples was analyzed by scanning electron microscope (SEM) coupled to an energy dispersive spectrometer (EDS) using Quanta 600 FEI-Philips equipment, operating at 25 kV. The gold coating was applied to the surface of the sample for this analysis.

4 RESULTS AND DISCUSSIONS

Figure 2 presents the transmission electron microographies of carbon nanotubes CNT₁, which shows in Figure 2a the presence of large agglomerates of nanotubes, with dimensions of 14 and 23 µm. Near this large particle, it is possible to observe a smaller particle of nanotube agglomerates with a diameter around 2 µm. A tangle of carbon nanotubes with a length around 6.5 µm can also be seen, as well as some individual fibers of carbon nanotubes with a size of 3.4 µm. Figure 2b and c show carbon nanotubes with lengths of 250 and 263 nm and diameters of 14 and 16 nm, respectively. Figure 3 presents the TEM microographies of carbon nanotubes CNT₂, which shows a similar agglomeration of carbon nanotubes. Here the carbon nanotubes have a length of around 3.26 and 1,06 µm and diameters varying from 47 to 69 nm. Figure 4 presents the TEM microographies of carbon nanotubes CNT₃, which in Figure 4a shows micrometric agglomerates of carbon nanotubes, as well as entangled fibers and individual particles of carbon nanotubes. The diameter of the carbon nanotubes varies from 37 to 39 nm. Considering the values of diameter and length declared by the supplier, there is a clear difference from the values observed in the TEM microographies for CNT₁ and CNT₂ carbon nanotubes. For carbon nanotubes CNT₃, the diameter values observed in the TEM images are in interval range declared by the supplier. According to the supplier, for values described in the Table 1, the length was obtained from high resolution transmission electron microscopy and the diameter was found from Raman spectroscopy. The particle sizes of three carbon nanotubes, namely diameter and length, were also observed in a previous publication [29]. As seen in the TEM images, the sonication process used for preparation of samples of carbon nanotubes for microscopy, or even possibly used by the supplier for dispersing them, resulted in breaking carbon nanotubes into small parts.

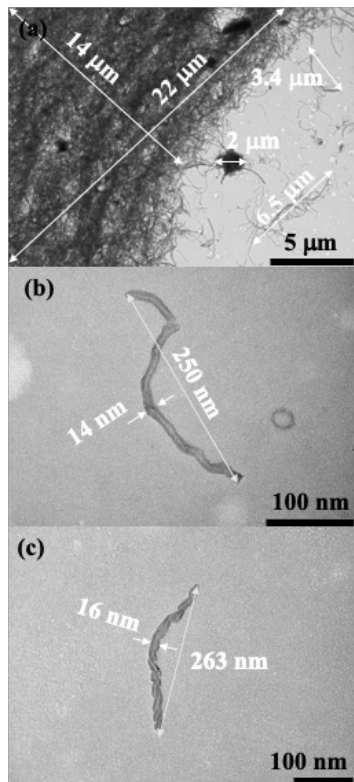


Figure 2. Transmission electron microographies of carbon nanotubes CNT₁

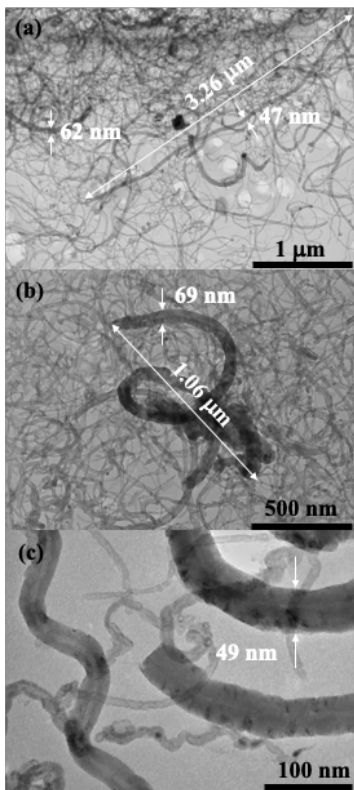


Figure 3. Transmission electron microographies of carbon nanotubes CNT₂

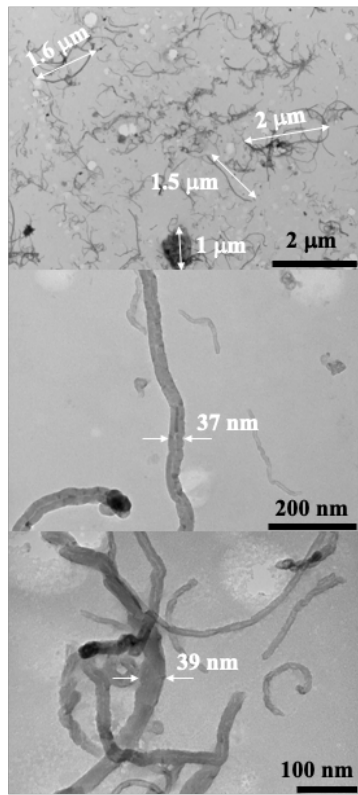


Figure 4. Transmission electron micrographies of carbon nanotubes CNT₃

Figures 5 presents the particle size distribution of carbon nanotubes and Portland cement obtained by laser granulometry. Carbon nanotubes have micrometric particles ranging from 1 to 100 μm and another population of particles smaller than 1 μm . CNT₁ is coarser than CNT₂ and CNT₃. Thus, considering the specific surface area of carbon nanotubes, it is verified in Table 1 that CNT₃ presented the highest SSA, while CNT₁ and CNT₂ presented similar values. The granulometry of carbon nanotubes before and after the ultrasonic dispersion was evaluated by Yakovlev et al. [25]. When in an agglomerated condition, nanotubes present the main volume of micrometric particles ($> 1 \mu\text{m}$), while the use of ultrasonic dispersion leads to the predominance of nanoparticles. The ultrasonic dispersion leads not only to a disentanglement of agglomerates of carbon nanotubes, but also to their rupture or breakage as reported by Hawreen et al. [18], [19] and Yakovlev et al. [25]. These two populations of particles, micrometric agglomerates or tangles of carbon nanotubes, are also observable in the TEM micrographies between 1 and 100 μm , as well as particles smaller than 1 μm , which are probably individual fibers of carbon nanotubes or pieces of them, resulting from the sonication process.

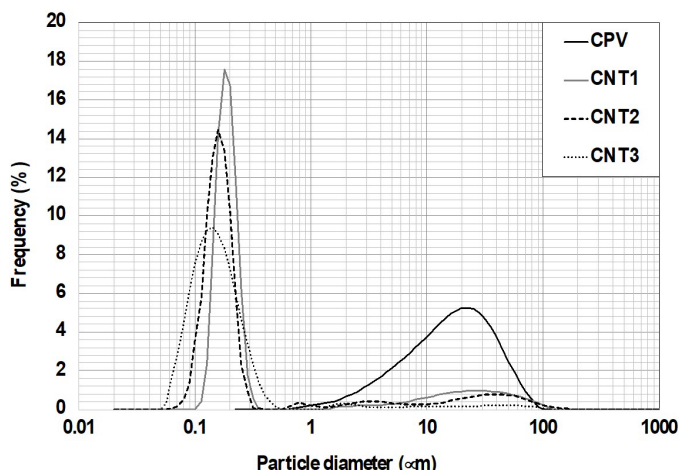


Figure 5. Particle size distribution Portland cement and carbon nanotubes

The laser granulometry test cannot assess the morphology of fibrous particles, such as diameter and length, even with equipment that combines laser granulometry and image analysis techniques. This technique provides information of the sizes of agglomerates or clamped particles, as well as dispersed carbon nanotubes and their small pieces, without a classification of their dispersion conditions [25], [26]. When combined with other techniques such as transmission electron microscopy and specific surface area, the laser granulometry test can help to understand how these particles affect the rheological behaviour of cementitious matrices [29]. Other techniques are available, such as UV-VIS spectroscopy [24], electro-acoustic attenuation spectroscopy [29], and LUMiSizer centrifugal methods [26].

Figure 6a shows the rheograms of reference paste and mixtures formulated with 0.1 and 0.2 wt% of CNT₁ carbon nanotubes. The Bingham Model was considered to fit a linear equation. The rheological behaviour was considerably altered due to the incorporation of carbon nanotubes in cementitious matrix. Table 4 lists the calculated volumetric concentration (V_S), volumetric surface area (VSA), porosity (P₀) and interparticle separation (IPS) calculations of the studied mixtures according to Funk and Dinger [30], and the yield stress and viscosity of cement pastes obtained from the Bingham model. Figure 6b shows the correlation between the interparticle separation (IPS) and yield stress of mixtures, in which a good correlation can be obtained. The most probable effect of carbon nanotubes is to reduce the interparticle separation of these suspensions, resulting in an exponential increase in yield stress, which is inversely proportional to interparticle separation IPS ($1/IPS^2$) [31]. Regarding the yield stress, the volumetric surface area (VSA) can be pointed as the main variable responsible for this rheological property. While the viscosity of suspensions is mainly affected by the increase of the solid concentration (V_S), which changed from 47.14% to 47.16%, viscosity does not present a good correlation with the Interparticle Separation (IPS).

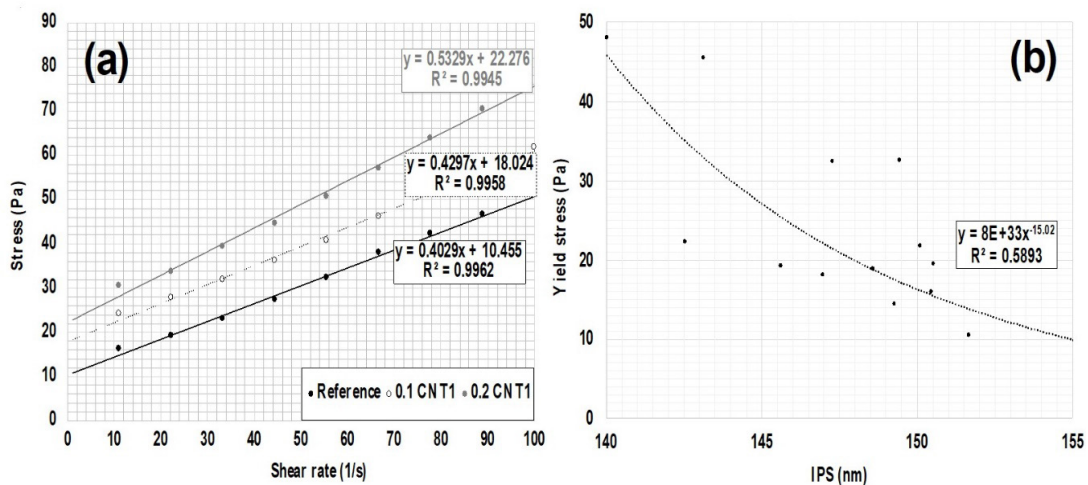


Figure 6. (a) Rheograms of mixtures (b) Effect of Interparticle separation (IPS) on the yield stress

Table 4 - Rheological properties of mixtures

Properties	V _S (%)	VSA (m ² /cm ³)	P ₀ (%)	IPS (nm)	τ_0 (Pa)	η (Pa.s)
Reference	47.14	4.24	32.33	151.66	10.45	0.36
0.025% CNT ₁	47.14	4.27	32.35	150.46	15.85	0.44
0.05% CNT ₁	47.15	4.30	32.36	149.28	14.35	0.35
0.1% CNT ₁	47.15	4.37	32.40	146.97	18.02	0.43
0.2% CNT ₁	47.16	4.49	32.46	142.55	22.27	0.53
0.025% CNT ₂	47.14	4.27	32.35	150.54	19.42	0.41
0.05% CNT ₂	47.15	4.30	32.37	149.44	45.46	0.49
0.1% CNT ₂	47.15	4.35	32.41	147.29	32.44	0.45
0.2% CNT ₂	47.16	4.47	32.48	143.14	32.52	0.63
0.025% CNT ₃	47.14	4.27	32.34	150.72	21.71	0.50
0.05% CNT ₃	47.15	4.32	32.37	148.59	18.76	0.43
0.1% CNT ₃	47.15	4.40	32.41	145.63	19.16	0.44
0.2% CNT ₃	47.16	4.56	32.48	140.03	47.96	0.36

V_S – solids content – VSA – Volumetric surface area – P₀ – calculated porosity – IPS – Interparticle separation - average flexural strength τ_0 - yield stress – η – viscosity

The type and content of surfactant was also cited as a variable responsible to the rheological change in cement formulated with carbon nanotubes [5], [6]. However, a similar increase of the rheological properties was observed by Batiston et al. [7] and Medeiros et al. [8] for mixtures containing carbon nanotubes, which used samples of carbon nanotubes in a powdered form without a surfactant agent for dispersing the carbon nanotubes. A polycarboxylate acid was used as a dispersing agent in both cases. Thus, considering the high amount of dispersing lignosulphonate employed here (1 wt%), which also acts as an entrapped air agent, and the lower dosage of surfactant in a mmol fraction, these same rheological properties, yield stress and viscosity, do not present a good correlation with the content of surfactant (Table 2).

The mechanical properties of mixtures formulated with carbon nanotubes CNT₁, CNT₂ and CNT₃ were also listed in Table 5. All mixtures have flexural strength values higher than reference. For mixtures containing carbon nanotubes CNT₁ and CNT₃, the maximum value was reached at 0.025 wt%. For CNT₂ carbon nanotubes, the optimal content, or the smallest quantity of nanotubes that led to the highest mechanical performance, was 0.05 wt%. Unlike the others, the flexural strength of CNT₂ carbon nanotubes increases after reaching the optimal content. Recently, a statistical study was published by Ramezani et al. [23], evaluating the large number of published studies on the use of carbon nanotubes in cement-based materials. Considering the flexural or tensile strength, the authors suggested an optimal content of 0.15 wt% of carbon nanotubes. For an experimental approach in the same study, they reached an optimal content of 0.1 wt% of carbon nanotubes, considering the flexural strength.

Figure 7a presents the stress (f_{tm}) x deflection (δ) curves of all evaluated samples. For the reference mixture, the typical behaviour of brittleness was identified. A maximum deflection (δ_{max}) of 0.2287 mm was achieved for this cementitious matrix. When 0.025 wt% of CNT₁ was added to this cementitious matrix, one of the six samples presented a higher deformation capacity. A maximum deflection (δ_{max}) of 0.4612 mm was observed, and the inclination of initial part of stress x deflection curve showed a reduction compared to the other samples. These two differences suggest a typical composite behaviour for this sample. The tenacity of this sample reached 1.88 J, considerably higher than the average value of 0.79 for mixtures containing 0.025 wt% of CNT₁ and listed in Table 5. A similar change in deformability of the same samples was observed for other mixtures formulated with CNT₁, as seen in Figure 7c, d and e. Figure 7f presents the typical behaviour of the reference mixtures and all samples containing CNT₁, which present the behaviour of a composite. A type of “plasticity” was verified in some stress x deflection curves, which can be attributed to the sample cracking and the performance of carbon nanotubes as a reinforcing material.

The same approach was considered for the mixtures formulated with carbon nanotubes CNT₂ and CNT₃, which are showed in Figures 8 and 9. There are many samples for different contents of carbon nanotubes, which present a typical composite behaviour. The behaviour of a composite type was mainly observed in Figure 8f, Figure 9f and Figure 7f. Thus, there is a higher probability of obtaining a composite type behaviour for CNT₂ (12/24), followed by a smaller probability for CNT₃ (7/24) and the least probability for CNT₁ (5/24). According to Callister [32], a minimum critical length was required when fibers are added into a matrix (Equation A).

Table 5 - Mechanical properties of mixtures

Properties	f_{tm} (MPa)	Tenacity (J)	E_d (GPa)	δ_{MAX} (mm)
Reference	5.89 +/- 0.68	0.50 +/- 0.20	29.22 +/- 0.58	0.2287
0.025% CNT ₁	7.53 +/- 1.50	0.79 +/- 0.57	29.78 +/- 0.30	0.4612
0.05% CNT ₁	6.86 +/- 1.61	0.84 +/- 0.23	29.95 +/- 1.42	0.4262
0.1% CNT ₁	6.35 +/- 1.14	0.75 +/- 0.38	28.31 +/- 0.78	0.3937
0.2% CNT ₁	6.68 +/- 0.81	0.76 +/- 0.60	28.52 +/- 1.25	0.4512
0.025% CNT ₂	6.02 +/- 0.55	0.62 +/- 0.32	30.38 +/- 1.07	0.3012
0.05% CNT ₂	7.28 +/- 0.85	1.01 +/- 0.23	30.03 +/- 1.95	0.3762
0.1% CNT ₂	6.92 +/- 1.17	0.71 +/- 0.27	29.80 +/- 2.61	0.3413
0.2% CNT ₂	7.81 +/- 2.13	1.14 +/- 0.51	30.92 +/- 0.71	0.4325
0.025% CNT ₃	7.80 +/- 1.58	0.88 +/- 0.41	29.98 +/- 2.55	0.3063
0.05% CNT ₃	6.33 +/- 0.83	0.62 +/- 0.27	30.03 +/- 2.31	0.3312
0.1% CNT ₃	5.98 +/- 2.14	0.46 +/- 0.17	28.28 +/- 2.05	0.2062
0.2% CNT ₃	6.92 +/- 0.99	0.68 +/- 0.20	28.71 +/- 0.93	0.3012

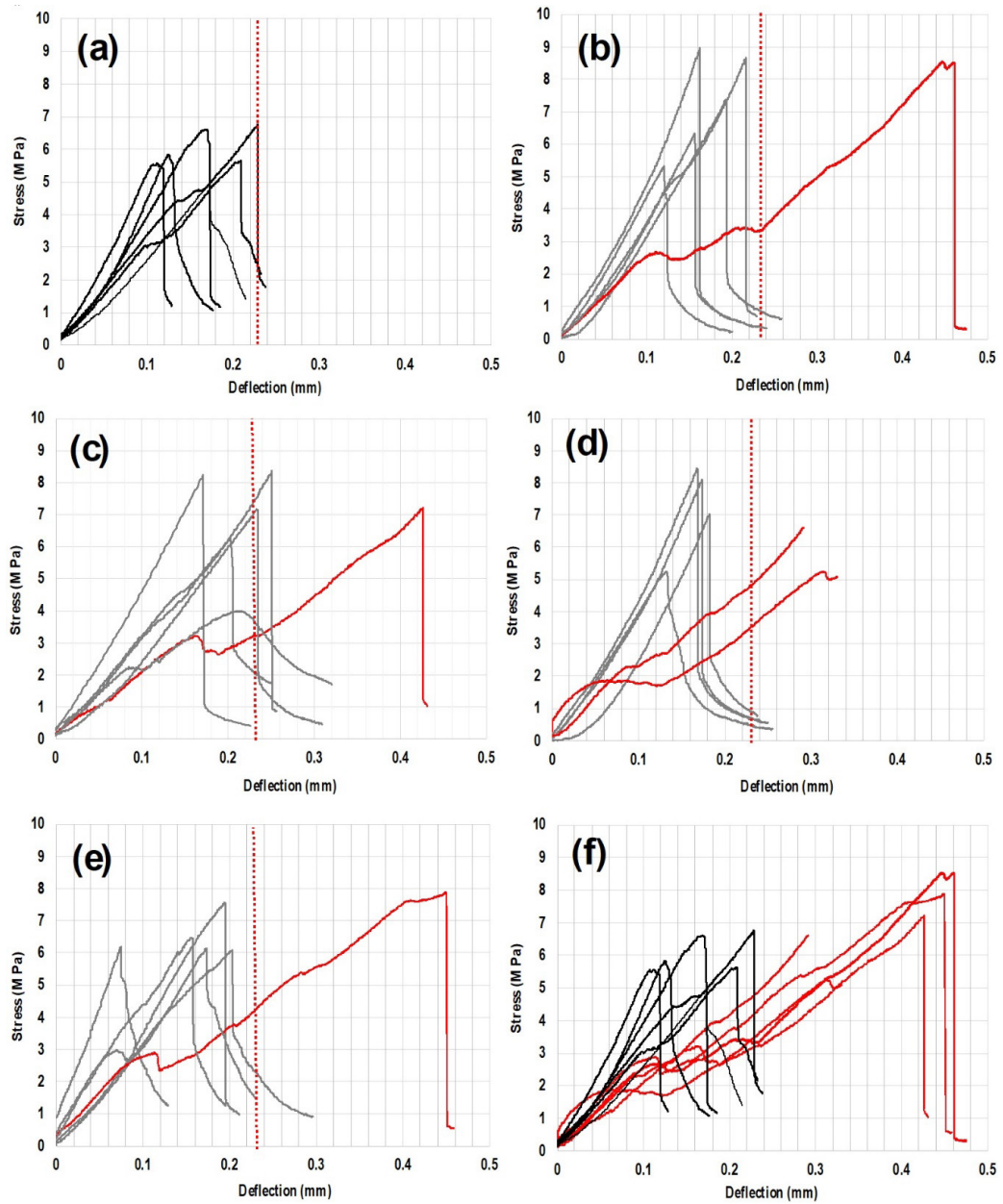


Figure 7. Stress x deflection of flexural tests (a) Reference (b) 0.025 wt.% CNT₁ (c) 0.05 wt.% CNT₁ (d) 0.1 wt.% CNT₁ (e) 0.2 wt.% CNT₁ (f) Reference and composite's samples containing CNT₁

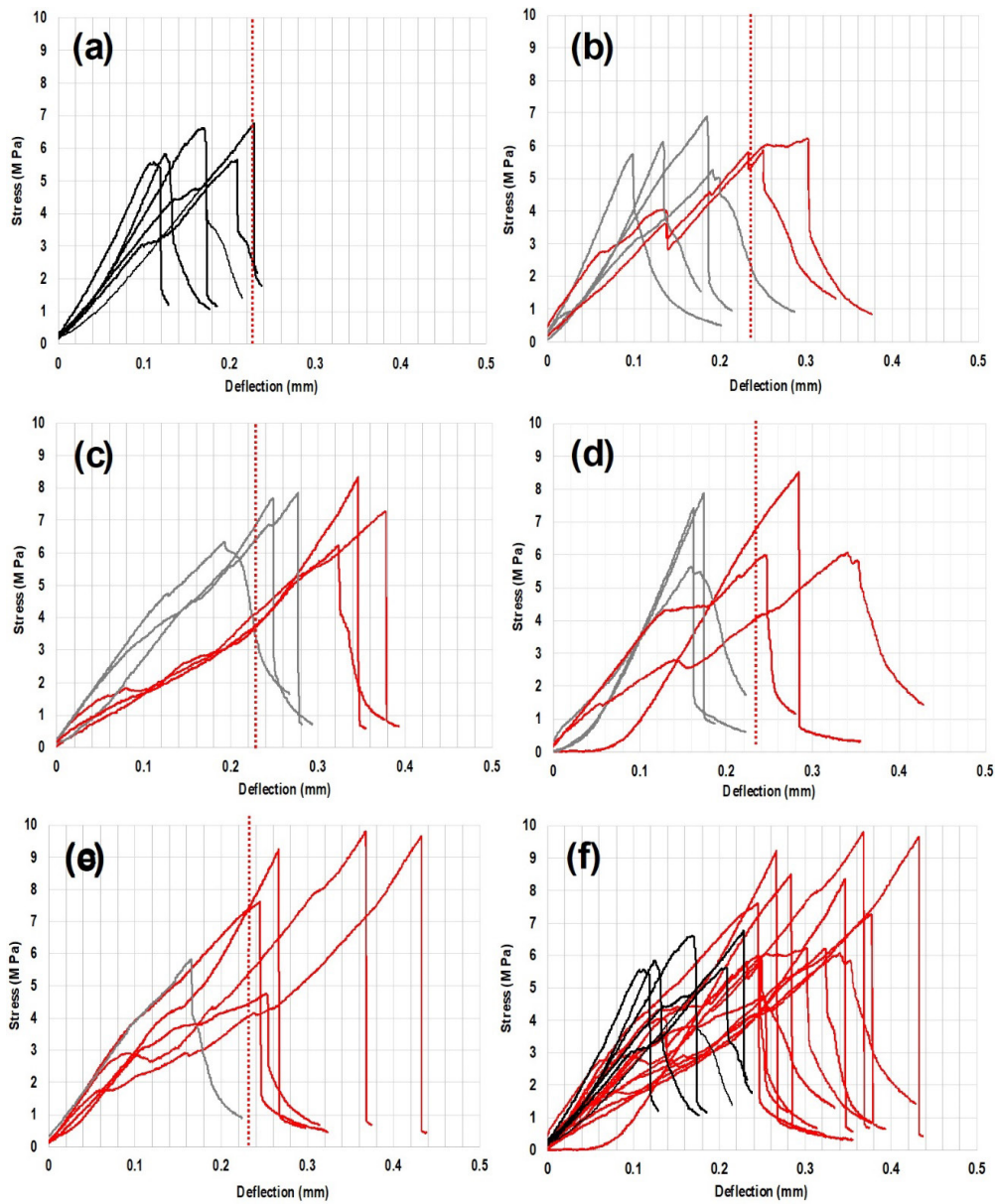


Figure 8. Stress x deflection of flexural tests (a) Reference (b) 0.025 wt.% CNT₂ (c) 0.05 wt.% CNT₂ (d) 0.1 wt.% CNT₂ (e) 0.2 wt.% CNT₂ (f) Reference and composite's samples containing CNT₂

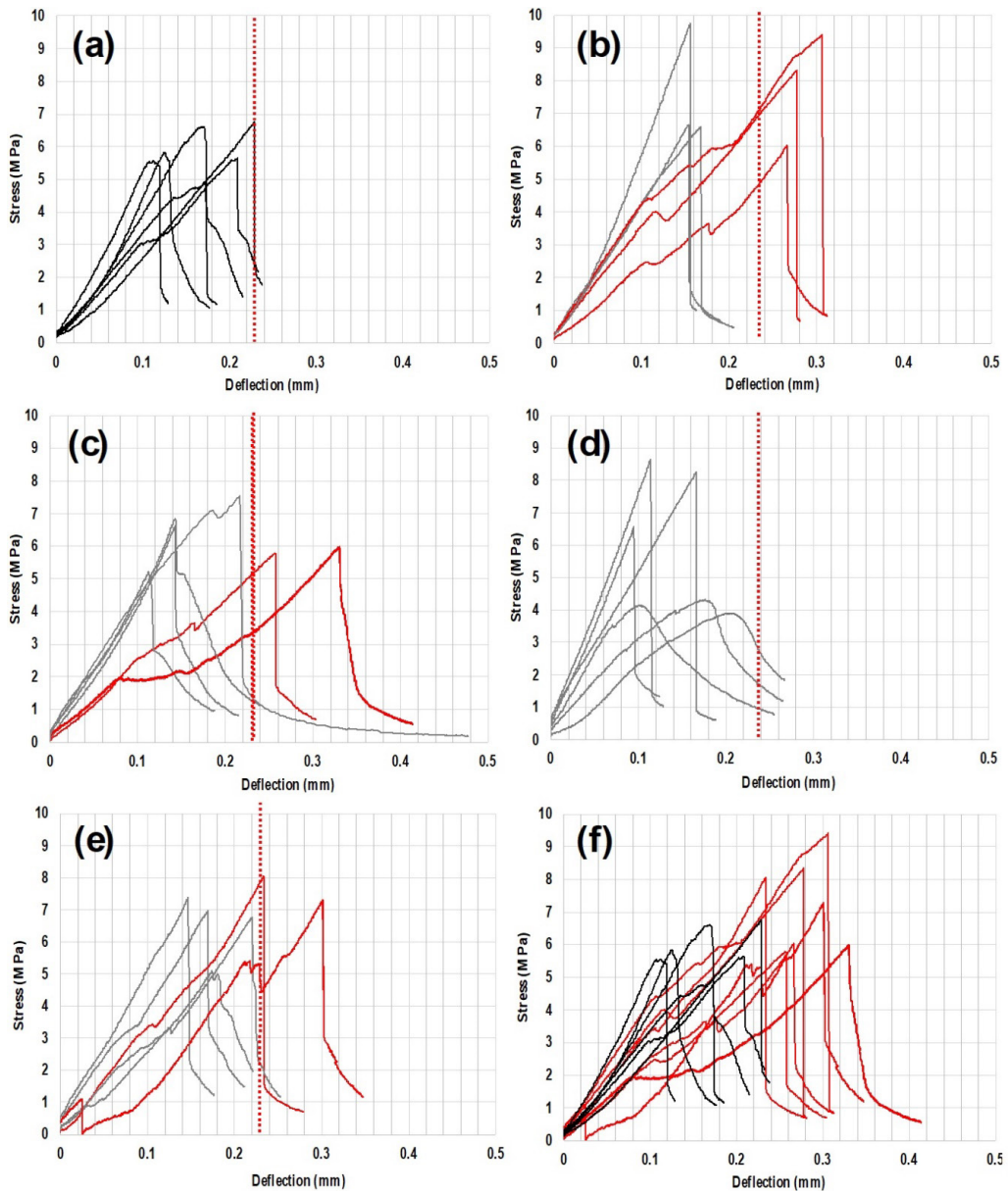


Figure 9. Stress x deflection of flexural tests (a) Reference (b) 0.025 wt.% CNT₃ (c) 0.05 wt.% CNT₃ (d) 0.1 wt.% CNT₃ (e) 0.2 wt.% CNT₃ (f) Reference and composite's samples containing CNT₃

Considering that the length (l_c), the diameter (d) and the tensile strength of carbon nanotubes (σ_f) are chosen, this last one can be considered equal to 850 MPa [33] or kept constant. The matrix strength (σ_m) or the adherence strength between carbon nanotubes and cementitious matrix is the only variable considered, which is proportional to its tensile strength. Peyvandi et al. [34] evaluated the effect of cementitious paste density, and consequently strength, on the performance efficiency of carbon nanofibers. The authors demonstrated that the efficiency of carbon nanofiber reinforcement was improved when the mechanical strength of cementitious matrix was increased. To assess how the adherence strength influenced the reinforcement efficiency of carbon nanotubes in cement-based materials, an efficiency factor called reinforced efficiency (R_E) can be estimated by Equation B. This is given by the ratio between the adherence strength (σ_m) required from Equation A, and the tensile strength of reference mixture without carbon nanotubes ($\sigma_{REF} = 5.89$ MPa). Table 6 presents the calculated values for CNT₁, CNT₂ and CNT₃, considering their geometric characteristics.

$$l_c = [(\sigma_f \cdot d) / (2 \cdot \sigma_m)]$$

Equation A

$$R_E = (\sigma_{REF} / \sigma_m)$$

Equation B

Table 6 - Geometric and adherence strength properties of carbon nanotubes

Properties	CNT ₁	CNT ₂	CNT ₃
l _c (micra)	15	20	15
d (nm)	50	25	40
l/d	300	800	375
σ _f (MPa)	850	850	850
σ _m (MPa)	1.416	0.531	1.133
R _E	5.89/1.416= 4.15	5.89/0.531= 11.08	5.89/1.133= 5.19

Figure 10a presents the probability of occurrence of similar composite behaviour for different Reinforced efficiency (R_E) values, which are indirectly related to the aspect ratio of carbon nanotubes. As the adherence mechanism is improved due to the geometric characteristics of carbon nanotubes, the probability of occurrence of behaviour similar to composite increases. In the mixtures formulated with CNT₂, which presented the best adherence mechanism between fiber and cementitious matrix, the probability of occurrence of behaviour similar to composite also increases according to CNT₂ content, as shown in Figure 10b. For the other carbon nanotubes, this relationship between fiber volume and composite like behaviour was not identified.

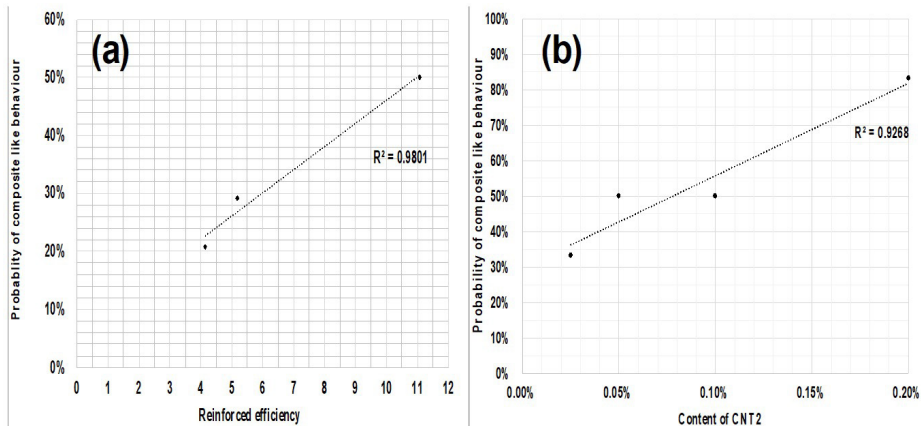
**Figure 10.** Probability of composite like behaviour as function of (a) Reinforced efficiency (b) volume of carbon nanotubes CNT2

Figure 11 shows the effects of carbon nanotubes on the hydration of Portland cement pastes containing 0.2 wt% of carbon nanotubes CNT₁, CNT₂ and CNT₃, named C01, C02 and C03. The thermogravimetric analysis of these mixtures showed that the composition C01 presents the highest mass loss, followed by compositions C03 and C02. Considering the mass loss between 100 and 400°C, which represents the calcium silicate and aluminate hydrates (C-S-H/C-A-H) [27], the mixtures C01, C03 and C02 showed values of 8.4, 7.8 and 5.2%, respectively. As for calcium hydroxide content, for temperatures ranging from 400 to 600°C [27], these formulations showed a mass loss of 4.7, 3 and 2.3%, respectively. For temperatures above 600°C [27], the decarbonation of calcium carbonate showed similar values ranging from 11.1 to 12.1%.

Figure 12 shows the diffractogram of composites C01, C02 and C03, containing 0.2 wt% of carbon nanotubes CNT₁, CNT₂ and CNT₃. Considering the C₃S peaks at $2\theta = 29.5^\circ$, the highest consumption of this phase was observed for the composite C01, followed by C02 and C03, respectively. Consequently, an inverse trend was observed for the main calcium hydroxide peaks at $2\theta = 34.1^\circ$. These results revealed that the increase in flexural strength observed for these formulations was not related to hydration products, since the C02 mixture, which presented the highest flexural strength, had the lowest mass loss for the hydration products. Likewise, the C02 mixture, which presents the highest flexural strength, did not present the maximum consumption of C₂S/C₃S phases, or the lowest peak for these phases. Recently,

Fehervari et al. [21] revealed that mechanisms for improved strength of mortars formulated with carbon nanofibers were not related to the hydration products. For higher dosages of carbon nanofibers (1 wt%), as compared with the values considered here, authors reported no difference on the porosity of mixtures formulated with or without these nanoparticles. The obtained results indicate that the geometric characteristic of carbon nanotubes can be pointed as an important issue. This approach of considering the aspect ratio and mechanical performance was also used by Hawreen et al. [19] and Batiston et al. [7]. For mixtures containing 0.1 wt% of carbon nanotubes with different aspect ratios, they showed that flexural strength was improved as the aspect ratio of carbon nanotubes increases.

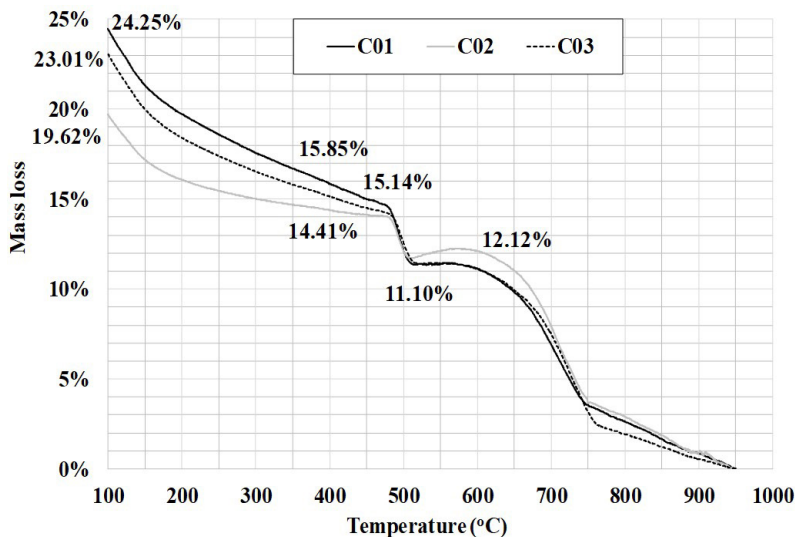


Figure 11. Thermo-gravimetric analysis of composites C01, C02 and C03

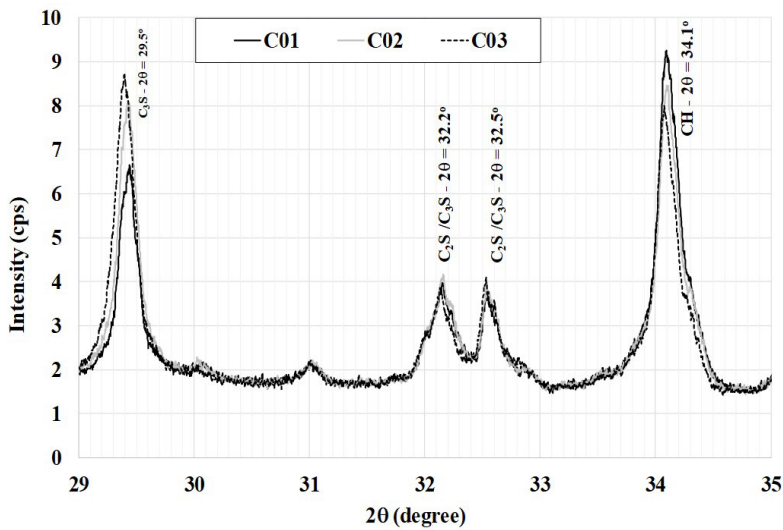


Figure 12. Diffractograms of composites C01, C02 and C03

Figure 13a shows a clear increase of diameter of the carbon nanotubes due to the growth of hydration products on the surface of nanoparticles. Figure 13b shows that the carbon nanotubes are entrapped into the hydration products. Figure 13c shows one carbon nanotube adhered on the surface of a cement particle, with the longest length covered by hydration products. Figure 13d shows many carbon nanotubes in a pore of the cementitious matrix, and the indication of the growth of a hydration product due to the nucleation effect of carbon nanotubes.

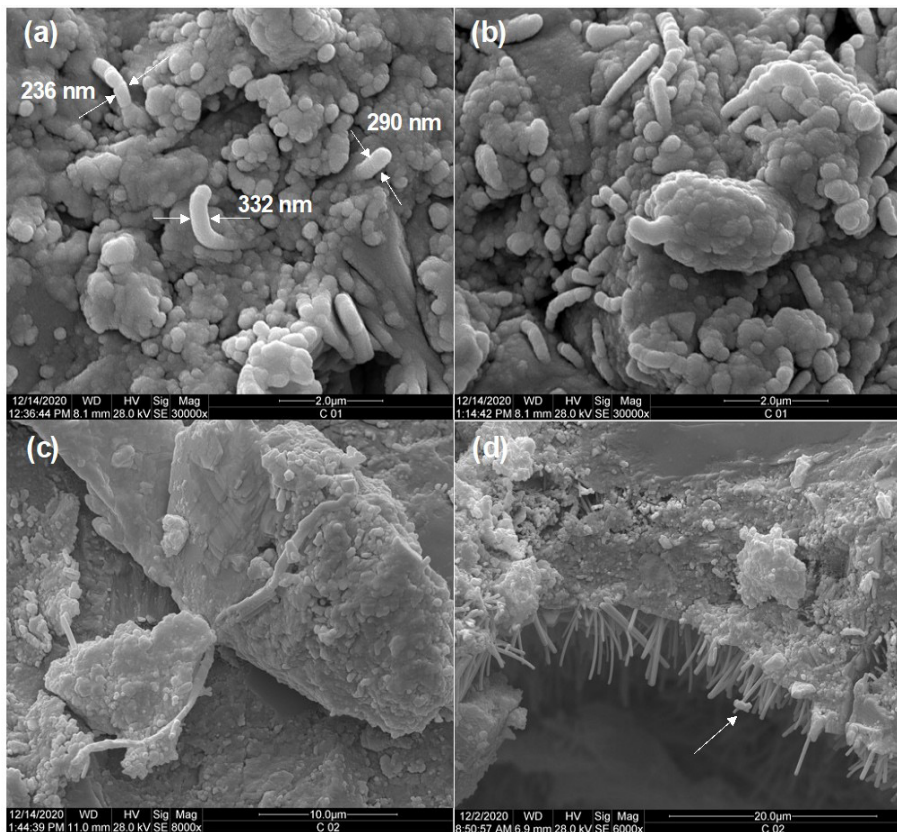


Figure 13. Scanning electron microographies of carbon nanotubes in Portland cement matrix

4 CONCLUSIONS

Carbon nanotubes affect the rheological properties of the Portland cement matrix. The high specific surface area of nanoparticles led to a reduction of the interparticle separation, and, consequently, to increasing the yield stress and viscosity of suspensions.

The mechanical performance is improved due to the incorporation of carbon nanotubes into the Portland cement matrix. A composite like behaviour was observed, which is directly related to the geometric characteristics of these nanoparticles.

The microstructural analysis showed that the geometric characteristics of carbon nanotubes do not change the hydration of these composite materials. The nucleation of hydration products takes place on the surface of carbon nanotubes.

ACKNOWLEDGEMENTS

The authors acknowledge the Araucaria Foundation, Coordination for the Improvement of Higher Education Personnel (CAPES) and National Council of Scientific and Technological Development (CNPq). LabMult UTFPR – Londrina.

REFERENCES

- [1] G. Y. Li, P. M. Wang, and X. Zhao, "Mechanical behavior and microstructure of cement composites incorporating surface treated multi-walled carbon nanotubes," *Carbon*, vol. 43, no. 6, pp. 1239–1245, 2005, <http://dx.doi.org/10.1016/j.carbon.2004.12.017>.
- [2] G. Yakovlev, J. Keriene, A. Gailius, and I. Girniere, "Cement based foam concrete reinforced by carbon nanotubes," *Medziagotyra*, vol. 12, no. 2, pp. 147–151, 2006.
- [3] M. S. Konsta-Gdoutos, Z. S. Metaxa, and S. P. Shah, "Highly dispersed carbon nanotube reinforced cement-based materials," *Cement Concr. Res.*, vol. 40, no. 7, pp. 1052–1059, 2010, <http://dx.doi.org/10.1016/j.cemconres.2010.02.015>.
- [4] J. S. Andrade No., T. Santos, S. A. Pinto, C. M. R. Dias, and D. V. Ribeiro, "Effect of the combined use of carbon nanotubes (CNT) and metakaolin on the properties of cementitious matrices," *Constr. Build. Mater.*, vol. 271, pp. 121903, 2021, <http://dx.doi.org/10.1016/j.conbuildmat.2020.121903>.

- [5] O. A. M. Reales, Y. P. A. Jaramillo, J. C. O. Botero, C. A. Delgado, J. H. Quintero, and R. D. Toledo Fo., "Influence of MWCNT/surfactant dispersions on the rheology of Portland cement pastes," *Cement Concr. Res.*, vol. 107, pp. 101–109, 2018, <http://dx.doi.org/10.1016/j.cemconres.2018.02.020>.
- [6] O. A. M. Reales, P. Duda, and R. Dias Toledo Filho, "Effect of a carbon nanotube/surfactant aqueous dispersion on the rheological and mechanical properties of portland cement pastes," *J. Mater. Civ. Eng.*, vol. 30, no. 10, pp. 04018259, 2018, [http://dx.doi.org/10.1061/\(ASCE\)MT.1943-5533.0002452](http://dx.doi.org/10.1061/(ASCE)MT.1943-5533.0002452).
- [7] E. Batiston, P. J. P. Gleize, P. Mezzomo, F. Pelisser, and P. R. Matos, "Effect of Carbon Nanotubes (CNTs) aspect ratio on the rheology, thermal conductivity and mechanical performance of Portland cement paste," *Rev. IBRACON Estrut. Mater.*, vol. 14, no. 5, e14510, 2021, <http://dx.doi.org/10.1590/s1983-41952021000500010>.
- [8] M. H. F. Medeiros, F. Dranka, A. J. Mattana, and M. R. M. M. Costa, "Portland cement composites with carbon nanotubes (CNT) addition: properties in freshly state and compressive strength," *Rev. Materia*, vol. 20, no. 1, pp. 127–144, 2015, <http://dx.doi.org/10.1590/S1517-707620150001.0014>.
- [9] S. Jiang et al., "Rheological properties of cementitious composites with nano/fiber fillers," *Constr. Build. Mater.*, vol. 158, pp. 786–800, 2018, <http://dx.doi.org/10.1016/j.conbuildmat.2017.10.072>.
- [10] M. S. Konsta-Gdoutos, Z. S. Metaxa, and S. P. Shah, "Multi-scale mechanical and fracture characteristics and early-age strain capacity of high-performance carbon nanotube/cement nanocomposites," *Cement Concr. Compos.*, vol. 32, no. 2, pp. 110–115, 2010, <http://dx.doi.org/10.1016/j.cemconcomp.2009.10.007>.
- [11] S. Musso, J. M. Tulliani, G. Ferro, and A. Tagliaferro, "Influence of carbon nanotubes structure on the mechanical behavior of cement composites," *Compos. Sci. Technol.*, vol. 69, no. 11–12, pp. 1985–1990, 2009, <http://dx.doi.org/10.1016/j.compscitech.2009.05.002>.
- [12] R. K. A. Al-Rub, A. I. Ashour, and B. M. Tyson, "On the aspect ratio effect of multi-walled carbon nanotubes reinforcements on the mechanical properties of cementitious nanocomposites," *Constr. Build. Mater.*, vol. 35, pp. 647–655, 2012, <http://dx.doi.org/10.1016/j.conbuildmat.2012.04.086>.
- [13] Z. Chen, J. L. G. Lim, and E. Yang, "Ultra-high-performance cement-based composites incorporating low dosage of plasma synthesized carbon nanotubes," *Mater. Des.*, vol. 108, pp. 479–487, 2016, <http://dx.doi.org/10.1016/j.matdes.2016.07.016>.
- [14] F. Collins, J. Lambert, and W. H. Duan, "The influences of admixtures on the dispersion, workability and strength of carbon nanotube-OPC paste mixtures," *Cement Concr. Compos.*, vol. 34, no. 2, pp. 201–207, 2012, <http://dx.doi.org/10.1016/j.cemconcomp.2011.09.013>.
- [15] F. Gao, W. Tian, Z. Wang, and F. Wang, "Effect of diameter of multi-walled carbon nanotubes on mechanical properties and microstructure of the cement-based materials," *Constr. Build. Mater.*, vol. 260, pp. 120452, 2020, <http://dx.doi.org/10.1016/j.conbuildmat.2020.120452>.
- [16] A. Sobolkina et al., "Dispersion of carbon nanotubes and its influence on the mechanical properties of the cement matrix," *Cement Concr. Compos.*, vol. 34, no. 10, pp. 1104–1113, 2012, <http://dx.doi.org/10.1016/j.cemconcomp.2012.07.008>.
- [17] D. J. Souza, L. Y. Yamashita, F. Dranka, M. H. F. Medeiros, and R. A. Medeiros-Junior, "Repair mortars incorporating multiwalled carbon nanotubes: shrinkage and sodium sulfate attack," *J. Mater. Civ. Eng.*, vol. 29, no. 12, 2017, [http://dx.doi.org/10.1061/\(ASCE\)MT.1943-5533.0002105](http://dx.doi.org/10.1061/(ASCE)MT.1943-5533.0002105).
- [18] A. Hawreen, J. A. Bogas, and A. P. S. Dias, "On the mechanical and shrinkage of cement mortars reinforced with carbon nanotubes," *Constr. Build. Mater.*, vol. 168, pp. 459–470, 2018, <http://dx.doi.org/10.1016/j.conbuildmat.2018.02.146>.
- [19] A. Hawreen, J. A. Bogas, M. Guedes, and M. F. C. Pereira, "Dispersion and reinforcement efficiency of carbon nanotubes in cementitious composites," *Mag. Concr. Res.*, vol. 71, no. 8, pp. 408–423, 2019, <http://dx.doi.org/10.1680/jmacr.17.00562>.
- [20] T. Manzur, N. Yazdani, and M. B. Emon, "Effect of carbon nanotube size on the compressive strengths of nanotube reinforced cementitious composites," *J. Mater.*, vol. 2014, pp. 960984, 2014, <http://dx.doi.org/10.1155/2014/960984>.
- [21] A. Fehervari et al., "On the mechanisms for improved strengths of carbon nanofiber-enriched mortars," *Cement Concr. Res.*, vol. 136, pp. 106178, 2020, <http://dx.doi.org/10.1016/j.cemconres.2020.106178>.
- [22] S. J. Chen, W. Wang, K. Sagoe-Crentsil, F. C. X. L. Zhao, M. Majumderc, and W. H. Duan, "Distribution of carbon nanotubes in fresh ordinary Portland cement pastes: understanding from a two-phase perspective," *RSC Advances*, vol. 6, no. 7, pp. 5745–5753, 2016, <http://dx.doi.org/10.1039/C5RA13511G>.
- [23] M. Ramezani, Y. H. Kim, and Z. Sun, "Z. Sun Z. Mechanical properties of carbon-nanotube-reinforced cementitious materials: database and statistical analysis," *Mag. Concr. Res.*, vol. 72, no. 20, pp. 1047–1071, 2020, <http://dx.doi.org/10.1680/jmacr.19.00093>.
- [24] L. Silvestro et al., "Influence of ultrasonication of functionalized carbon nanotubes on the rheology, hydration, and compressive strength of Portland cement pastes," *Materials*, vol. 14, no. 18, pp. 5248, 2021, <http://dx.doi.org/10.3390/ma14185248>.
- [25] G. I. Yakovlev et al., "Modification of cement matrix using carbon nanotubes dispersion and nano-silica," *Procedia Eng.*, vol. 172, pp. 1261–1269, 2017, <http://dx.doi.org/10.1016/j.proeng.2017.02.148>.
- [26] B. Krause, M. Mende, P. Pötschke, and G. Petzold, "Dispersability and particle size distribution of CNTs in an aqueous surfactant dispersion as a function of ultrasonic treatment time," *Carbon*, vol. 48, no. 10, pp. 2746–2754, 2010, <http://dx.doi.org/10.1016/j.carbon.2010.04.002>.
- [27] H. F. W. Taylor, *Cement Chemistry*. London: Academic Press, 1990, 451 p.

- [28] American Society for Testing and Materials, *Standard Test Method for Dynamic Young's Modulus, Shear Modulus, and Poisson's Ratio by Impulse Excitation of Vibration*, E1876, 2009.
- [29] T. M. Mendes and W. L. Repette, "Carbon nanotubes added to Portland cement matrices containing nanosilica," *Acta Scientiarum*, vol. 2, pp. 1, 2022.
- [30] J. E. Funk and D. Dinger, *Predictive Process Control of Crowded Particulate Suspension*. Massachusetts: Springer, 1994, 786 p.
- [31] R. J. Flatt and P. Bowen, "Yodel: a yield stress model for suspensions," *J. Am. Ceram. Soc.*, vol. 89, no. 4, pp. 1244–1256, 2006, <http://dx.doi.org/10.1111/j.1551-2916.2005.00888.x>.
- [32] W. D. J. Callister, *Fundamentals of Materials Science and Engineering*. Rio de Janeiro: LCT, 2006.
- [33] H. Kim et al., "Tensile properties of millimeter-long multi-walled carbon nanotubes," *Sci. Rep.*, vol. 7, no. 1, pp. 9512, 2017, <http://dx.doi.org/10.1038/s41598-017-10279-0>.
- [34] A. Peyvandi, L. A. Sbia, P. Soroushian, and K. Sobolev, "Effect of the cementitious paste density on the performance efficiency of carbon nanofiber in concrete nanocomposite," *Constr. Build. Mater.*, vol. 48, pp. 265–269, 2013, <http://dx.doi.org/10.1016/j.conbuildmat.2013.06.094>.

Author contributions: T.M.M.: conceptualization, data curation, formal analysis, methodology, writing; M.H.F.M: funding acquisition, revision, supervision.

Editors: Fernando Pelisser, Guilherme Aris Parsekian.